

Transversally and longitudinally stiffened steel plate girders subjected to patch loading

Rolando Chacón, Enrique Mirambell, Esther Real

Department of Civil and Environmental Engineering, Universitat Politècnica de Catalunya, Barcelona, Spain

Revision submitted to and accepted in THIN WALLED STRUCTURES 2019

Abstract

This article presents some observations related to the phenomenon that occurs when transversally and longitudinally stiffened steel plate girders are subjected to patch loading. The failure mechanism differs considerably for the particular structural case of girders with largely spaced transverse stiffeners, which have been studied thoroughly in last decades. Steel plate girders with closely spaced stiffeners are occasionally found in bridge design and for such cases, the current EN1993-1-5 rules underestimate the strength of the webs to transverse forces. Research work on girders with closely spaced transverse stiffeners is available but for such cases, the web plates are longitudinally unstiffened. Some comparisons between the results obtained and those provided by EN1993-1-5 are discussed. Preliminary results suggest that the resistance of densely stiffened steel girders (both transversally and longitudinally) must be studied and subsequently revised accordingly. In addition, it is pointed out that a certain degree of imperfection sensitivity is inferred from the results. Further studies on this topic are necessary.

Keywords: Patch loading; EN1993-1-5; Stiffening, longitudinal stiffening, plate buckling

1. Introduction

Steel plate girders have been studied profusely in last decades. The usage of such structures in the civil engineering world is vast: countless examples of steel and composite bridges as well as a great number of buildings worldwide are nowadays totally or partially assembled with steel girders. Steel plate girders are designed with either symmetric, non-symmetric I-sections or with a different configurations of box girders.

In bridges, I-shaped steel girders are routinely assembled with slender plates for the webs (relatively high values of h_w/t_w) and with stocky flanges (low values of b_f/t_f). This combination leads to a high flexural capacity for a relatively low weight. There are, however, issues concerning the stability of the plates assembling the girders. Occasionally, these elements must be stiffened both transversally and longitudinally by welding additional plates that enhance the overall as well as the local behaviour of these elements. From the design perspective, girders assembled with stocky web plates may lead to less stiffening (reducing the labour cost associated with welding but increasing the total weight and the cost associated with the material). Conversely, slender web plates may lead to lighter structures. For an adequate design, these plates often need to be stiffened for the sake of accomplishing all ultimate and serviceability limit states. Constructional guides covering the vast majority of topics dealing with stability and plate girders have been presented by Dowling et al. [1], Galambos [2], Dubas and Gehri [3] and Beg et al. [4].

In bridges assembled with the incremental launching method, patch loading has been identified as one major verification to be considered at design stages. Launching minimizes the use of heavy equipment but implies that all cross-sections of the plate girder pass over temporary supports or piers. Thus, concentrated forces act in both transversally stiffened and unstiffened sections. Occasionally, the thickness of the web (t_w) is governed by a temporary concentrated load during the launching operation. An alternative to increasing the web thickness is to stiffen

the web plate with equally spaced vertical stiffeners or a combination of vertical and longitudinal elements. Although longitudinal elements are initially conceived for bending and shear capacity, they provide an enhancement to the overall resistance of the plates towards several buckling phenomena.

Extensive experimental, numerical and theoretical investigations related to patch loading in both unstiffened and longitudinally stiffened panels have been published. Summary works related to this topic have been presented by Lagerqvist and Johansson [5-6], Chacón et al. [7] and Graciano [8]. From these summaries, a fourfold conclusion (illustrated in Fig. 1) can be extracted:

- In unstiffened panels or panels with largely spaced transverse stiffeners, the failure mode of steel plate girders subjected to patch loading is related to **web folding** under the concentrated load. The ultimate load capacity primarily depends on the web strength as well as on the flange stiffness. The mechanical behaviour of longitudinally unstiffened panels with largely spaced transverse stiffeners is well known. Most predictions found in structural codes are reliable and based upon simple yet accurate formulations derived from mechanical models.
- In girders with closely spaced transverse stiffeners, the failure mode is associated with an intertwined mechanism of **web folding and flange yielding**. The ultimate load capacity primarily depends on the web strength and the flange strength. For the particular case of closely spaced transverse stiffeners, research has been active rather recently and guidelines do not provide an explicit theoretical treatment to those cases. The definition of the distance between transverse stiffeners as large or close is particularly crucial for the definition of the patch loading resistance. Largely spaced transverse stiffeners do not contribute to the resistance to patch loading whereas closely spaced elements allow a considerable redistribution of stresses within the loaded panels at high load levels. Previous works presented by the authors [9-11] show that for girders with aspect ratios $a/h_w=1,0$ (a relatively frequent proportion in bridge design), their resistance to patch loading is considerably enhanced by the presence of such elements.
- In longitudinally stiffened panels, **web folding** under the concentrated load is observed. The ultimate load capacity of longitudinally stiffened elements also depends on the position and the rigidity of the longitudinal stiffener and it is generally higher than the ultimate load capacity of an equivalent member with no longitudinal stiffening. Web folding may be observed in the directly loaded panel or in its vertically adjacent subpanel. Sequential research performed by Graciano et al. [12-15] and Kövesdi et al. [16-17] depicts both critical buckling and ultimate resistance of such elements when subjected to patch loading.
- Research related to the particular case of members with longitudinal stiffening and closely spaced transverse elements is scant. Densely stiffened plates, which may provide a considerably high resistance to patch loading, have not yet been studied systematically. In recent years, research has been focused on other aspects of patch loading such as the behaviour of hybrid girders [18-19], eccentric patch loading [20-21] and practical applications for bridge construction [22-23].

In this paper, the previous study is generalized to the case of girders with considerable dense stiffening. Steel plate girders considering both longitudinal stiffeners as well as transverse elements designed with aspect ratios $a/h_w=1,0$ are studied. A set of variations of other geometrical proportions such as web slenderness h_w/t_w , the longitudinal stiffener position and rigidity and the flange yield stress f_{yf} are studied by means of a numerical parametric study. The study was performed using a commercial FE-package [24] following the recommendations

concerning the designer-assumed initial conditions on plate buckling problems provided in [25-26]. A phenomenological insight of the mechanical behaviour shows the potential stress redistribution and the potential contribution of the longitudinal stiffener.

2. EN1993-1-5

The design load of plate girders subjected to concentrated loads (F_{Rd}) is included in the present version of EN1993-1-5 [27] in the same form as in other instability-related problems, i.e., the χ - λ approach as shown in equations (1) to (4). In this approach, the plastic strength F_y is partially reduced by a χ_F coefficient which takes instability into account. The effectively loaded length is defined as l_y . Note that the magnitude of l_y is limited to the distance between transverse stiffeners "a". If the calculated value " l_y " is greater than the geometrical value "a", the ultimate load carrying capacity given in EN1993-1-5 is proportionally reduced to this transverse spacing. On the other hand, regardless of the potential effect the stiffening may have in the calculation, l_y is independent of the presence/absence of longitudinal stiffeners. The benefits that the stiffening provides are implicitly included within the formulation via the buckling coefficient k_F (Eq. 5), in which distance "a", the position b_1 and the relative flexural-torsional rigidity γ_s are included.

$$F_{Rd} = \frac{F_{Rk}}{\gamma_{M1}} \quad (1)$$

$$F_{Rk} = \chi_F \cdot F_y = \chi_F \cdot f_{yw} \cdot l_y \cdot t_w \leq \chi_F \cdot f_{yw} \cdot a \cdot t_w \quad (2)$$

$$l_y = S_s + 2t_f \cdot \left(1 + \sqrt{m_1 + m_2}\right) = S_s + 2t_f \cdot \left(1 + \sqrt{\frac{f_{yf} \cdot b_f}{f_{yw} \cdot t_w} + 0,02 \cdot \left(\frac{h_w}{t_f}\right)^2}\right) \leq a \quad (3)$$

$$\chi_F = \frac{0.5}{\lambda_F} \quad \bar{\lambda}_F = \sqrt{\frac{F_y}{F_{cr}}} \quad F_{cr} = 0,9 \cdot k_f \cdot E \cdot \frac{t_w^3}{h_w} \quad (4)$$

$$k_{F,unstiffened} = 6 + 2 \cdot \left(\frac{h_w}{a}\right)^2 \quad (5)$$

$$k_{F,longitudinally\ stiffened} = 6 + 2 \cdot \left(\frac{h_w}{a}\right)^2 + \left[5,44 \frac{b_1}{a} - 0,21\right] \cdot \sqrt{\gamma_s}$$

A hypothetical analysis of such limitation is illustrated in Fig. 2. Assuming that all other variables are held constantly and varying systematically with the distance "a", one may find the following trend: the predicted strength reduces with the spacing between vertical stiffeners "a". A singular point occurs as expected when the geometrical distance "a" equals the calculated effectively loaded length l_y . The calculated values of F_{Rd} for a given girder are normalized to the obtained value when the girder presents stiffeners separated a long distance ($a \rightarrow \infty$). This seems to be counterintuitive to the stiffening philosophy, which suggest that more stiffening should lead to higher capacity of the loaded plates.

Nevertheless, the future generation of EN1993-1-5 will include an amended version of this formulation. The effectively loaded length l_y has been updated (AM-1-5-11-06) as reads in Eq. 6. Subsequently, the reduction factor was accordingly modified and standardized to other instability-related problems (Eq. 7 to 9). Additional details concerning this amendment as well as its statistical evaluation are provided in [7].

$$l_y = S_s + 2t_f \cdot (1 + \sqrt{m_1}) = S_s + 2t_f \cdot \left(1 + \sqrt{\frac{b_f}{t_w}}\right) \leq a \quad (6)$$

$$\chi_F = \frac{1,0}{\varphi_F + \sqrt{\varphi_F^2 - \bar{\lambda}_F}} \leq 1,0 \quad (7)$$

being

$$\varphi_F = \frac{1}{2} \left(1 + \alpha_{F0} \cdot (\bar{\lambda}_F - \bar{\lambda}_{F0}) + \bar{\lambda}_F\right) \quad (8)$$

$$\bar{\lambda}_F = \sqrt{\frac{I_y \cdot t_w \cdot f_{yw}}{F_{cr}}} \quad (9)$$

3. Proposed mechanism for girders with closely spaced transverse stiffeners subjected to patch loading

Experimentally and numerically, it has been found [9-11] that a typical response curve of girders with closely spaced stiffeners subjected to patch loading follows the qualitative shape illustrated in Fig. 3. Linear initial stages are followed by a bifurcation point in which folding of the web occurs. The system redistributes stresses and the formed web yield lines during folding are anchored in the transverse stiffeners. This anchorage promotes the development of tensile stresses in the web that generate four hinges in the loaded flange. F_1 has been identified as the load at which web folding occurs and ΔF_F as the additional load that may be carried by the flange while dissipating energy in the plastic collapse. Full collapse of the system occurs at F_2 .

A theoretical solution to the problem of web instability in plate girders with closely spaced vertical stiffeners under patch loading can be found in a predictive model based on two terms (Eq. 10) proposed in [9-10] and improved for practical applications in [11]. The first term contains the web contribution given in the EN1993-1-5 specification for $l_y=a$ (web folding of a panel whose width equals “a”). The second term is the corresponding contribution of the flange and it is designated as ΔF_F .

$$F_{Rk,proposed} = F_{Rk}^* = F_{Rk(l_y=a)} + \Delta F_F = \chi \cdot F_{y,(l_y=a)} + \Delta F_F = \chi \cdot f_{yw} \cdot a \cdot t_w + \Delta F_F \quad (10)$$

For the derivation of ΔF_F , a theoretical limit analysis over a defined yield mechanism is used. This mechanism involves the formation of four plastic hinges in the loaded flange of the steel plate girder. It is assumed that the web folds at a load of magnitude F_1 . Thus, further load increments are resisted by the loaded flange which acts as a flat-beam with cross-section $b_f \cdot t_f$ subjected to stresses due to bending. If the transverse stiffeners are rigid, the flat beam can be approximated as fully restrained element at both ends and the total length of this member equals to the distance between transverse stiffeners “a”. The flexural resistance of the flange is calculated with Eq. (11) and only the flange cross-section ($b_f \cdot t_f$) is considered to be effective in contributing to the strength. However, at load F_1 , when the frame mechanism is expected to begin, direct stresses are present in the flanges due to global bending. As a result, only a fraction of the nominal yield stress of the flange (f_{yf}) defined as f_{yf}^* , can be used in the calculation of the hinge resistance.

The magnitude of the flange reserve f_{yf}^* is the available strength on those elements when the applied patch load is equal to F_1 . At this point, the web buckles and the flanges are stressed to some extent due to global bending. The magnitudes of χ_{fi} and χ_{fo} are defined in Eq. (12) and represent the ratio of actual longitudinal stress in the flange (σ_{fi}) when compared to the nominal

flange yield stress f_{yf} . ΔF_F is subsequently defined in Eq. 13 as the capacity provided by a partially stressed flange. The magnitude of ΔF_F accounts for the flange contribution and is obtained using the principle of virtual work in which this partial stress level is included via the ratios χ_{fi} and χ_{fo} .

$$M_{yf} = \frac{1}{4} b_f \cdot t_f^2 \cdot f_{yf}^* \quad (11)$$

$$f_{yf,o}^* = (1 - \chi_{fo}) \cdot f_{yf} \quad f_{yf,i}^* = (1 - \chi_{fi}) \cdot f_{yf} \quad \chi_{fi} = \frac{\sigma_j}{f_{yf}} \left(1.0 + 0.005 \left(\frac{h_w}{t_w} \right) \right) \quad (12)$$

$$\Delta F_f = \frac{b_f \cdot t_f^2 \cdot f_{yf}}{(a - S_s)} \cdot [2 - (\chi_{fo} + \chi_{fi})] \quad (13)$$

$$k = \left[1.25 - 0.25 \cdot \left(\frac{f_{yf}}{f_{yw}} \right) \right] \quad (14)$$

It is worth noticing that the proposed ΔF_F capacity is implicitly dependent on the web slenderness. Slender girders provide a considerably higher hinge-based capacity when compared to stocky elements. This capacity is also proportionally defined by the available strength f_{yf}^* . For slender girders, F_1 is low, resulting in a high flange strength reserve. For stocky girders, F_1 is high, resulting in a low flange strength reserve. Additionally, for the sake of calibration, an empirically obtained coefficient including the web slenderness is defined in Eq. 12. Finally, the correction coefficient k (Eq. 14) has been proposed to account for the design of hybrid plate girders [28] since it has been also observed that an arbitrarily high value of f_{yf} does not provide an indefinitely high increment of the patch loading capacity.

4. Girders with longitudinal stiffeners

If the panel is longitudinally stiffened, the question is to know the influence of the position and/or the flexural-torsional rigidity of the longitudinal stiffener in the failure mechanism of the panel. The influence of the longitudinal stiffener on the resistance of plate girders subjected to patch loading has been generally approached from two perspectives:

- The panel is treated as unstiffened and subsequently, a “ f_s ” factor is defined. This factor increases the resistance of the unstiffened panel in a percentage, which is a function of the longitudinal stiffener itself and its position within the panel.
- The panel is treated as stiffened and as such, its geometrical conditions can be changed in the definition of F_{cr} . This approach also leads to a certain increment of F_{Rk} as a function of the stiffener and its position. Currently, EN1993-1-5 is based upon this approach. Eq. 5 defines a buckling coefficient accounting for the position b_1 and its corresponding flexural-torsional rigidity. Optimal values of longitudinal stiffeners rigidity have been proposed in the literature with satisfactory results [8]. Recent research [16] performed on longitudinally stiffened girders (some of them with closed-sections) includes modified versions of k_F with satisfactory results also.

One aspect that has been a matter of debate is the distance of the longitudinal stiffener to the loaded flange (b_1). While initially conceived for bending purposes, this proportion defines failure on the loaded panel. For some cases, failure is concentrated in the panel below the longitudinal stiffener (low values of b_1). For other cases, failure is concentrated in the panel above the longitudinal stiffener (high values of b_1). For other cases (weak longitudinal stiffeners, or particular positions), the observed failure mode is rather intertwined between panels.

5. Numerical model

The multi-purpose code Abaqus-Simulia [24] has been systematically used as a simulation tool in this research. The code has been widely contrasted and bench-marked in several plate-buckling related phenomena. The characteristics of the used numerical model read:

- Geometrically, the girders are idealized with S4 shell elements.
- Materially, the steel is idealized as elastic-plastic with a von Mises yield criterion. In the case of material idealization including strain hardening, an isotropic hardening model is used. Three different types of steel were modelled (S355, S460 and S690). In all cases, the material has been idealized as elastic-perfectly plastic with no strain hardening.
- The iterative procedure for solving the assembled equation is the Newton-Raphson method. The chosen incremental procedure is based upon the arc-length method.
- The stability analysis are performed following an eigenvalue extraction using a subspace procedure.

The reproduction of the patch loading phenomena is based upon additional assumptions such as mesh design, geometrical and structural imperfections of the girders. These assumptions are generally “designer-assumed”. Consequently, concerns about the reliability of such assumptions arise, particularly when large systematic parametric studies are developed. The idealization of the girders within this work has been based upon the recommendations provided by EN1993-1-5-Annex C. These rules provide guidance for using FE-analyses in the calculation of plated structures. The modelling may be either based upon a refined analysis by including geometrical imperfections (Eigenmode-based, for instance) and structural imperfections (residual stresses). Alternatively, it allows the usage of shapes based upon equivalent geometric imperfections.

In a series of research papers published by the authors for unstiffened girders, it is suggested that patch loading analysis can be based upon critical Eigenmodes of the structure conveniently scaled a maximum amplitude “ w ” [25]. EN1993-1-5-Annex C rules recommend a value for w at least of 80% of the maximum allowed fabrication tolerances (80%·FT). In addition, it is stated in EN1993-1-5-Annex C that the chosen imperfection shape should lead to the lowest resistance for each case. In the particular case of patch loading, the initial out-of-flatness of the web in the directly loaded panel should be the most significant initial imperfection. The refined analysis requires the numerical modelling of structural imperfections by means of a typical residual stress pattern [26].

Fig. 4 shows a typical shell-based idealization, the mesh (structured with S4R quadrilateral elements of approximate size 20mm) and the geometrical shape (Eigenmode-based) defined as initial imperfection. The defined geometry is a three-paneled girder that is simply supported along stiffened sections of the outer panels and loaded on the middle one. Fig. 5 shows results provided in [25] in which experimental and numerical values are compared. For the case of

longitudinally stiffened webs, similar results have been recently presented by other research groups [17].

6. Parametric study

The numerical model has been used systematically as a simulation tool in order to study steel plate girders subjected to patch loading. The main feature and novelty of this study is the presence of longitudinal stiffeners in girders with closely spaced transverse elements. Conclusions provided by prior studies suggest the following characteristics:

- The geometrical proportions that lead to the singular situation in which $a/l_y < 1,0$ are found in girders whose web height ranges from 500 mm to 2000 mm. Since longitudinal stiffener are used in this study, the numerical study is developed in girders with $h_w = a = 2000$ mm. The use of these longitudinal elements is justified in girders with considerable web height.
- Other proportions are chosen from according realistic dimensions of steel girders. The web slenderness is varied systematically for covering a broad range.
- The flange yield strength f_{yf} plays a primarily role in the development of the post- F_1 mechanism. Three values of f_{yf} are included in this study.
- All elements are designed with rigid flat longitudinal stiffeners whose dimensions are $b_{stl} \cdot t_{stl}$ (110mm·30mm) and are held constant.
- The position of the longitudinal stiffener ranges from $b_1/h_w = 0,2$ to $b_1/h_w = 0,3$ since these values represent the optimal limits for an effective design to bending.

The study includes variations of web thickness t_w , flange yield stress f_{yf} and the position of the longitudinal stiffener b_1 . It is worth pointing out that the flanges are defined as stocky elements and as such, the resistance to patch loading is not affected by any transverse bending of the flanges. Table 1 displays the set of variations as well as other magnitudes of interest. An extra set of girders following the same characteristics but longitudinally unstiffened is included for comparison purposes. A total amount of 20 Eigenvalue extractions (buckle) and 60 nonlinear analyses have been performed.

7. Results obtained

7.1 Results obtained with EN1993-1-5

Tables 2 to 5 display the results obtained in all specimens when applying the EN1993-1-5 formulation (based upon the amended formulae only, i.e., equations 6 to 9). Table 2 shows the results obtained for unstiffened girders whereas Tables 3, 4 and 5 show the results obtained when varying $b_1 = 400$ mm; $b_1 = 500$ mm and $b_1 = 600$ mm respectively. The numbering of the

girders of each girder in all tables ranges from 1 to 15. Corresponding numbers in all tables are fully comparable (with the varying position as the main difference).

Closer inspection on the results obtained allow drawing the following observations:

- The calculated values of “ l_y ” are greater than “ a ” in girders with slender web plates. Strictly, these values are corrected as depicted in section 3. In stocky specimens ($t_w=12$ and $t_w=15$), “ l_y ” is smaller and this particular anomaly does not appear.
- The corrected value of l_y is independent from f_{yf} . According to EN1993-1-5, the resistance to patch loading F_{Rk} happens to be independent of this value.
- According to EN1993-1-5, for a given girder, all longitudinally stiffened elements provide a greater buckling load F_{cr} than their unstiffened counterparts do.
- According to EN1993-1-5, for a given girder, all longitudinally stiffened elements provide a greater resistance F_{Rk} than their unstiffened counterparts do.
- For both buckling (F_{cr}) and ultimate resistance (F_{Rk}), the difference between girders with varying position of the longitudinal element is not very high. The maximum value is consistently obtained for girders with $b_1=500\text{mm}$.

7.2 Eigenvalue extraction

An Eigenvalue extraction was performed in all specimens with varying geometry. These elements correspond to those labeled as [1;4;7;10;13] in tables 2 to 5. This extraction is elastic and thus independent of the yield stress of the plates assembling the girders. Table 6 displays frontal views of the 1st Eigenmode in 20 simulations. Numerical values are also included.

The following observations can be pointed out:

- Eigenmodes correspond to plate buckling of the loaded panels. These failure modes are associated to the patch loading phenomena and according to the conclusions presented in [25-26], may be used as a sound initial imperfection.
- In some cases ($b_1=600\text{mm}$), the shape involves both subpanels (above and below the longitudinal stiffener). This happens for the case of very stocky webs. An intertwined shape covering both subpanels is observed.
- The elastic critical buckling loads increase with the web thickness as expected and it is greater for longitudinally stiffened elements than for their unstiffened counterparts.
- The elastic critical buckling loads increases with b_1 .

7.3 Nonlinear analyses

Nonlinear analysis in all 60 configurations were performed. The obtained results are presented in the form of response curves for some representative cases. Noticeably, the model provides softening branches with considerable levels of deformation. In this study, plastic damage rules or fracture mechanics were not included in the model. Both extremes ($t_w=6\text{mm}$ and $t_w=15\text{mm}$) are analyzed in a detailed fashion.

7.3.1 Slender girders

Figures 6 to 9 show both response curves and graphical visualizations of the simulations ($t_w=6\text{mm}$) at key load levels. The influence of the position b_1 as well as the influence of the flange yield stress f_{yf} are assessed. According to the theoretical results, all girders would correspond to the case in which $a>l_y$. Plots are extracted for girders with $f_{yf}=355\text{N/mm}^2$.

Closer inspection on the results obtained for slender girders allow pinpointing:

- Longitudinally stiffened girders present a response curve with some similarities when compared to the unstiffened case. The load-displacement curve shows a lost in linearity which is followed by a post- F_1 branch suggesting a change in the resistant mechanism. At a certain value F_2 , the load-bearing capacity is exhausted.
- The position b_1 changes, however, key aspects of such plots. For instance, the cases of $b_1=400\text{mm}$ and $b_1=500\text{mm}$ present a singular drop in the load-displacement curve. The load increases after some increments following a behavior usually observed in imperfection-sensitive structures.
- The overall behavior for $b_1=600\text{ mm}$ is similar to the one observed in unstiffened girders.
- The von Mises stresses at F_1 show that a considerable concentration of stresses is located on the directly loaded panel. Since the initial imperfection is related to the panel below the longitudinal stiffener (see table 6), one may expect folding in such panel as well.
- The value of F_1 is independent from f_{yf} (similarly to unstiffened elements) but the value of F_2 is considerably dependent of this magnitude.
- The von Mises stresses at F_2 also show that a considerable concentration of stresses is located on the directly loaded panel. In this plot, the deformed scale illustrates the hogging-and sagging shape of the loaded flange at this load level.
- In all slender girders, strains did not exceeded at 100mm displacement. The study was not concerned with potential excessive straining.

For the longitudinally stiffened cases ($b_1=400\text{mm}$ and $b_1=500\text{mm}$), the results suggest that the imperfection may play a role worth investigating. Figure 10 shows contours of the out-of-plane displacement for girders at F_1 . It shows that for all the studied positions b_1 , both subpanels are deformed perpendicularly. Although one may not be conclusive with the presented results, this figure provides hints about the shape of the webs at F_1 when compared to the shape of the webs at F_2 displayed in previous figures.

7.3.2 Stocky girders

Figures 11 to 14 show both response curves and graphical visualizations of the simulations. The influence of the position b_1 as well as the influence of the flange yield stress f_{yf} are assessed. According to the theoretical results, none of these girders would correspond to the case in which $a>l_y$. Thus, the formulation would not need any revision. In these figures, the nomenclature used previously does not make any sense since neither clear point F_1 nor post- F_1 branches are observed. Plots associated with F_{\max} as well as hogging and sagging zones at high level of displacement are presented instead.

Closer inspection on the results obtained for slender girders allow pinpointing:

- In all cases, the load-displacement curve shows a lost in linearity which is followed by a softening branch.
- The position b_1 influences the value of F_{max} . The greatest value is achieved for the case of $b_1=400\text{mm}$ but this value is independent of f_{yf} .
- The von Mises stresses at F_{max} show that a considerable concentration of stresses is located on the directly loaded panel for all cases.
- The von Mises stresses at $\delta=50\text{mm}$ show the deformed scale, which also illustrates the hogging-and sagging shape of the loaded flange at this displacement level.
- The flange yield stress f_{yf} influences the softening branch at high values of displacement.
- In all stocky girders, the plastic strain on the flanges did not exceeded 5%. Thus, the study was not concerned with excessive straining.

7.3.3 Intermediate slenderness

Other results obtained show a response curve with a shape that suggests a higher dependency on the initial imperfection. As an example, Fig. 15 displays the plot for the case $t_w=10\text{mm}$ and $b_1=400\text{mm}$. The softening branch is initially very acute up to a certain level of displacement, where the hinge-mechanism seems to play role. More studies concerning the influence of imperfections on the response for these cases are necessary. A clear post- F_1 branch depending on f_{yf} is observed. However, the acute drop in the load after F_1 undermines the strength reserve that is provided by the flange in the case of unstiffened cases. Clarification concerning this topic is needed. The designer-assumed conditions that have been validated for unstiffened webs may not be valid for transversally and longitudinally stiffened elements. Before activating the post- F_1 reserve, a snap-back phenomenon that must be analyzed is observed. This topic seems to be dependent on modelling (geometrical and/or structural imperfection sensitivity) and requires further clarification.

7.4 Numerical vs. EN1993-1-5 results

Another source of comparison would be the ratio between the obtained numerical values $F_{2,num}$ and the characteristic EN1993-1-5 load capacity F_{Rk} in its present form. Preliminary results (before performing a deeper imperfection analysis) show that the set of girders in which the effectively loaded length is greater than the distance between transverse stiffeners “a” are considerably safe-sided. Figure 16 displays this ratio as a function of the web slenderness. It is noticeable how the proportion $F_{2,num}/F_{Rk}$ increases with h_w/t_w . Since ΔF_F is higher for slender girders, higher scatter and difference with the current EN1993-1-5 guidelines are obtained. The results for stocky girders are similar to those observed in other statistical evaluations of girders subjected to patch loading since for those cases, the post- F_1 mechanism is not activated [7]. Another interesting plot is shown in Fig. 17, in which these ratios are presented as a function of b_1 . On average, a visual inspection of this plot suggests that these ratios decrease with distance b_1 . This underestimation is particularly noticeable in girders with higher f_{yf} in the loaded flange. However, the strength reserve provided by the flange for the case of unstiffened elements is not fully observed in longitudinally stiffened elements (for the case of intermediate slenderness).

8. Conclusions

In this paper, a new formulation for steel plate girders subjected to patch loading previously proposed by the authors is revisited for potential application in the particular case of girders with both transversal and longitudinal stiffening. Multiple conclusions can be drawn from this study:

- In its present form, EN-1993-1-5 provisions for steel girders with closely spaced transverse stiffeners underestimate the ultimate load capacity observed numerically. The results obtained herein reinforce those derived by the authors in previous publications.
- Numerical results confirm previous findings for longitudinally stiffened girders which provide a greater resistance to patch loading than unstiffened webs.
- When transversally stiffened, longitudinally stiffened girders with slender webs present a similar behavior than their unstiffened counterparts with a considerable contribution of the flange in the collapse mechanism. The case of stocky webs also shows a similar behavior in which in relative terms, the flange contribution is negligible.
- The proposed model for unstiffened girders seems to be adequate for longitudinally stiffened elements. For those girders in which the conditions are fulfilled, the response follows qualitatively the same trend. There is a dependency on F_1 that seems to be influenced by the position b_1 . Further studies are necessary in order to harmonize the model for unstiffened elements to the studied case.
- The girders with intermediate web slenderness show a response curve that needs revision in terms of the adopted initial imperfection. For the sake of generalizing the potential use of the proposed model in longitudinally stiffened elements, further studies concerning this topic are mandatory. Thus, the model presented in section 3 is not fully applicable in its present form. Clarification of the snap-back phenomenon is needed before providing more generality.

9. References

- [1] Dowling P., Harding J., Bjorhovde R., *Constructional Steel Design. An international guide*, Elsevier applied science, London and New York. 1992.
- [2] Galambos T., *Guide to Stability design criteria for metal structures*, John Wiley and sons New York. 1998.
- [3] Dubas P., Gehri E. *Behaviour and design of steel plated structures*, ECCS-CECM-EKS Zurich. 1986.
- [4] Beg D., Kuhlmann U., Davaine L., Braun B., *Design of Plated Structures: Eurocode 3: Design of Steel Structures, Part 1-5*. Ernst & Sohn, Berlin. 2012.
- [5] Lagerqvist O., Johansson B. "Resistance of I-girders to concentrated loads" *Journal of Constructional Steel Research*. **39**(1), 87-119. 1996
- [6] Lagerqvist O., Johansson B. "Resistance of plate edges to concentrated forces". *Journal of Constructional Steel Research*, **32**, 69 – 105, 1995

- [7] Chacón, R., Braun B., Kuhlmann U., Mirambell E., "Statistical evaluation of the new resistance model of steel plate girders subjected to patch loading". *Steel Construction*. **5** (1). 10-15. 2012
- [8] Graciano C. "Patch loading resistance of longitudinally stiffened webs- A systematic review". *Thin-walled Structures*. **95**(10). 1-6. 2015
- [9] Chacón R., Mirambell E., Real E. "Transversally stiffened plate girders subjected to patch loading. Part 1. Preliminary study". *Journal of Constructional Steel Research*, **80**(1). 483-491. 2013.
- [10] Chacón R., Mirambell E., Real E. "Transversally stiffened plate girders subjected to patch loading. Part 2. Additional numerical study and design proposal". *Journal of Constructional Steel Research*, **80**(1). 492-504. 2013
- [11] Chacón R., Herrera J., Fargier-Gabaldón L. "Improved design of transversally stiffened steel plate girders subjected to patch loading". *Engineering Structures*. **150**(11). 774-785. 2017
- [12] Graciano C., "Ultimate resistance of longitudinally stiffened webs subjected to patch loading". *Thin-Walled Structures*. **41**(6). 529-541. 2003
- [13] Graciano C., Johansson B. "Resistance of longitudinally stiffened I-girders subjected to concentrated loads". *Journal of constructional Steel Research*. **59**(5). 561-586. 2003
- [14] Loaiza N., Graciano C., Casanova E. "Design recommendations for patch loading resistance of longitudinally stiffened I-girders". *Engineering Structures*. **171** (10). 747-758. 2018
- [15] Loaiza N., Graciano C., Chacón R. "Web crippling strength of longitudinally stiffened steel plate girders webs to concentrated loads". *Engineering Journal, American Institute of Steel Construction*. **55** Q3. 191-201. 2018
- [16] Kövesdi B. "Patch loading resistance of slender plates with longitudinal stiffeners". *Journal of Constructional Steel Research*. **140**. 237-246. 2018
- [17] Kövesdi B. Mecséri B.J., Dunai L. "Imperfection analysis on the patch loading resistance of girders with open section longitudinal stiffeners". *Thin-Walled Structures*. **123**(2). 195-205. 2018
- [18] Chacón R., Mirambell E., Real E. Hybrid steel plate girders subjected to patch loading, Part 1: Numerical study. *Journal of Constructional Steel Research*, **66** (5) 695-708. 2010
- [19] Chacón R., Mirambell E., Real E. Hybrid steel plate girders subjected to patch loading, Part 2: Design proposal. *Journal of Constructional Steel Research*, **66** (5) 709-715. 2010
- [20] Šćepanović B., Gil-Martín L., Hernandez-Montes E., Aschheim M., D. Lučić D. "Ultimate strength of I-girders under eccentric patch loading: Derivation of a new strength reduction coefficient". *Engineering Structures*. **31**(7), 1403-1413. 2009
- [21] Uribe-Henao A. Graciano C. "Strength of steel I-girders subjected to eccentric patch loading". *Engineering Structures*. **79**. 401 - 406. 2014
- [22] Chacón R., Zorrilla R. "Structural Health Monitoring in Incrementally Launched Bridges: Patch Loading Phenomena Modeling". *Automation in Construction*. **58**. 60-73. 2015
- [23] Navarro-Manso A., del Coz Díaz J., Alonso-Martínez M., Blanco-Fernández E., Castro-Fresno D. "New launching method for Steel bridges based on a self-supporting deck system: FEM and DOE analyses". *Automation in Construction*. **44**(8). 183-196. 2014
- [24] Abaqus-Simulia v. 6.16. Dassault Systèmes. 2016
- [25] Chacón R., Mirambell E., Real E. "Influence of designer-assumed initial conditions on the numerical modeling of steel plate girders subjected to patch loading". *Thin-Walled Structures*. **47**(4). 391-402. 2009
- [26] Chacón R., Serrat M., Real E., "The influence of structural imperfections on the resistance of plate girders to patch loading". *Thin-Walled Structures*. **53**(4). 15-25. 2012

- [27] EN1993-1-5. Eurocode 3. Design of steel structures – Part 1-5: Plated structural elements CEN. 2006
- [28] Chacón R., Mirambell E., Real E., “Influence of flange strength on transversally stiffened girders subjected to patch loading”. *Journal of Constructional Steel Research*. **97**(4). 39-47. 2014

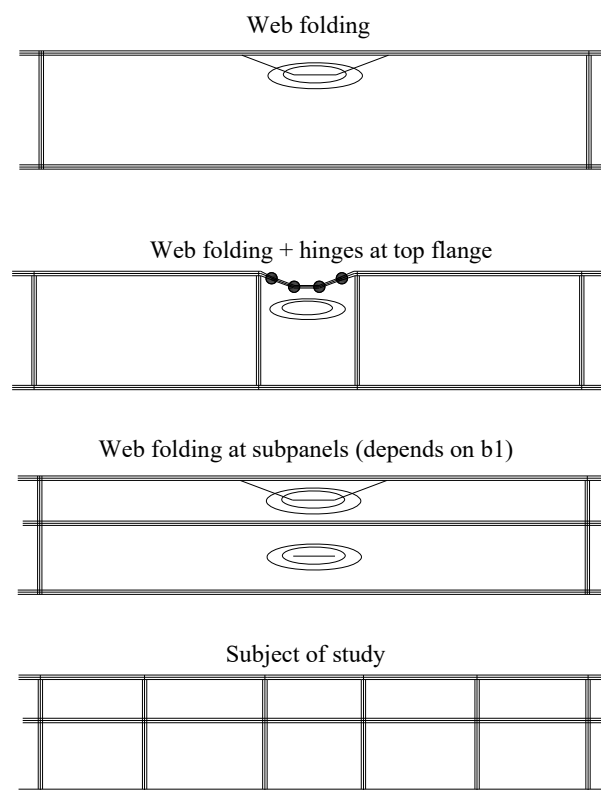


Figure 1. Typical failure modes in stiffened and unstiffened girders

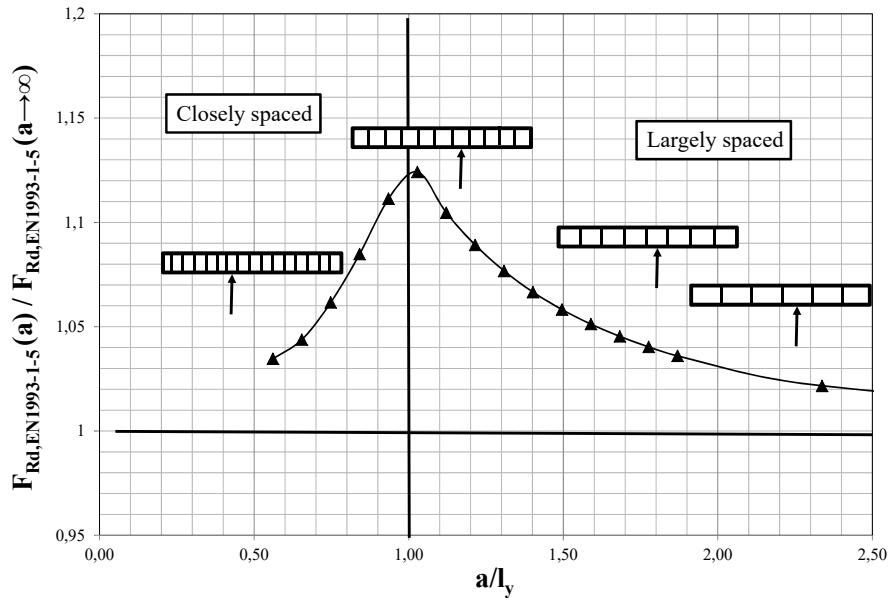


Figure 2. EN1993-1-5 resistance to transverse forces as a function of distance “a”

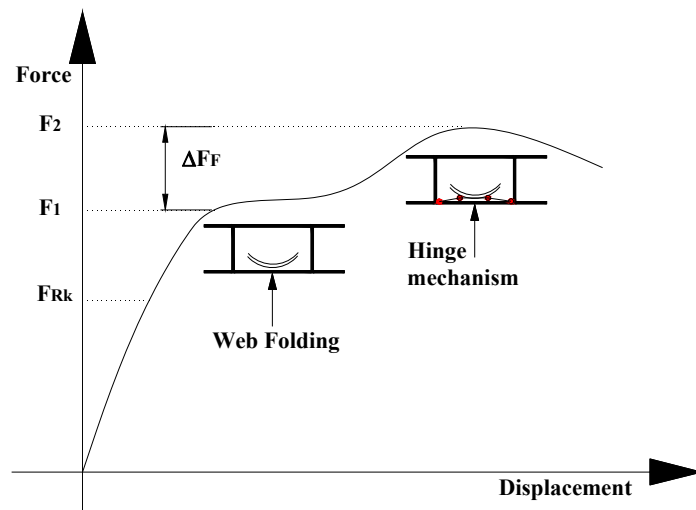


Figure 3. Load-displacement response plot for girders with closely spaced



Figure 4. Typical shell-based geometry, mesh and eigenmode-based imperfection.

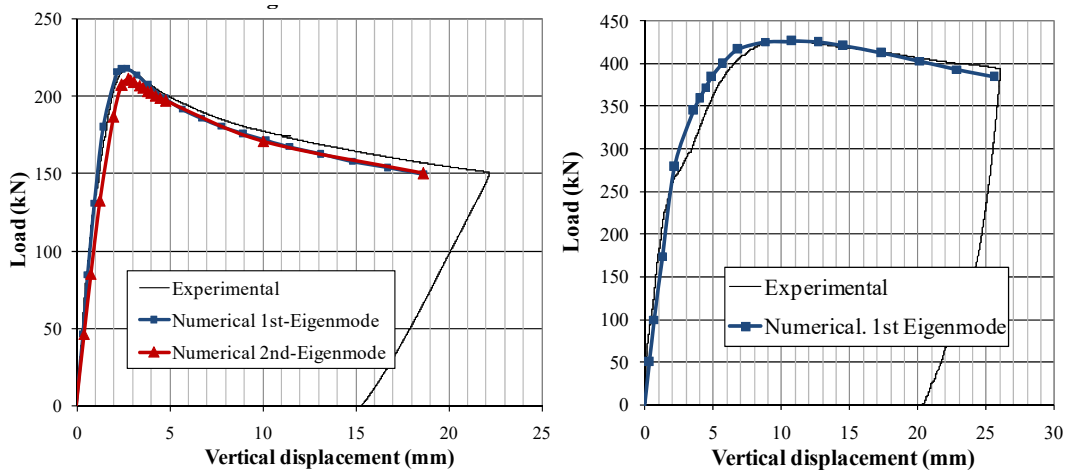
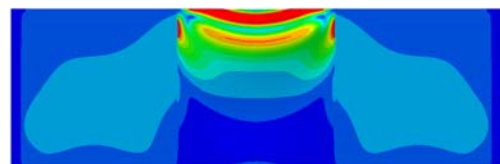
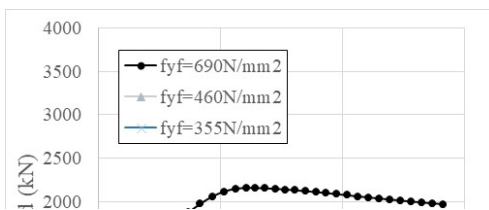
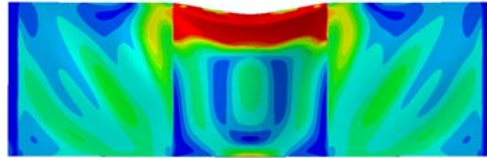


Figure 5. Validation of the numerical model [22]

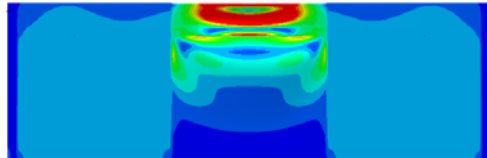
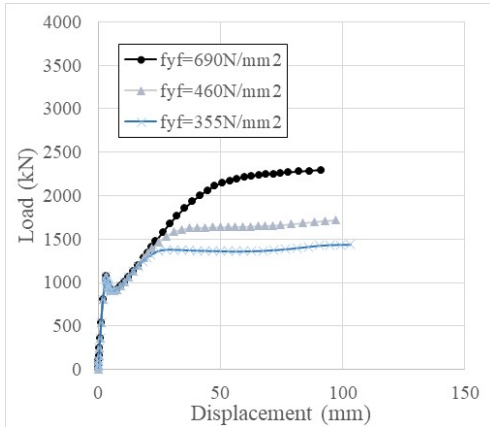


von Mises stresses at $F_1=840,1\text{ kN}$

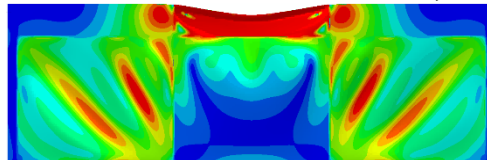


von Mises stresses at F_2

Figure 6. Unstiffened plates. Slender girders $t_w=6\text{mm}$

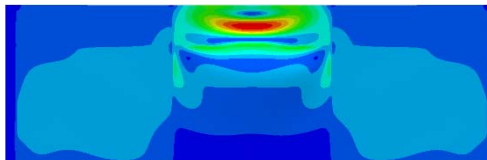
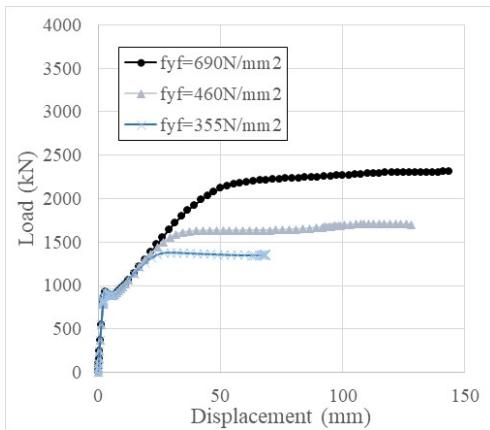


von Mises stresses at $F_1=1070,8\text{ kN}$

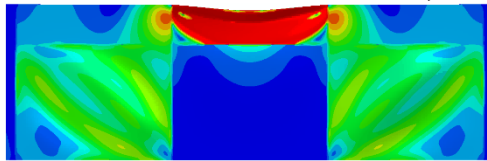


von Mises stresses at F_2

Figure 7. Longitudinally stiffened girders $b_1=400\text{mm}$. Slender girders $t_w=6\text{mm}$

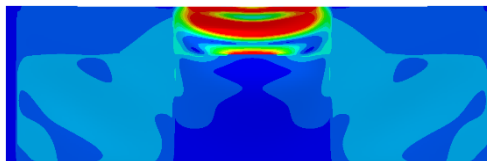
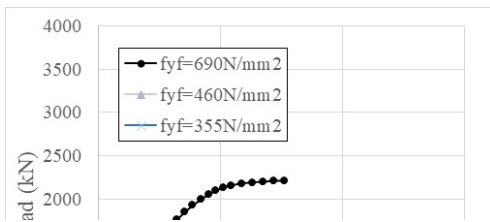


von Mises stresses at $F_1=929,9\text{ kN}$

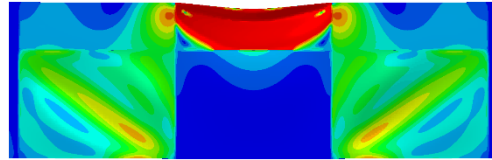


von Mises stresses at F_2

Figure 8. Longitudinally stiffened girders $b_1=500\text{mm}$. Slender girders $t_w=6\text{mm}$



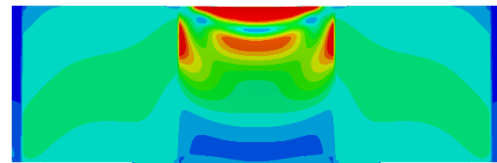
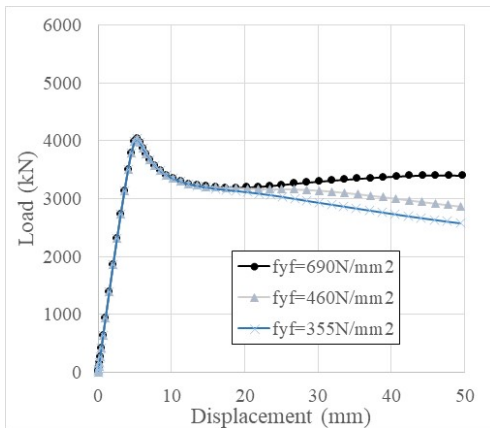
von Mises stresses at $F_1=862,8\text{ kN}$



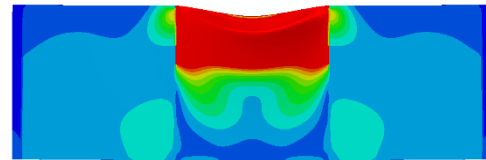
von Mises stresses at F_2
 Figure 9. Longitudinally stiffened girders $b_1=600\text{mm}$. Slender girders $t_w=6\text{mm}$



Figure 10. Out of plane displacement at F_1 for girders with varying $b_1=600\text{mm}$.

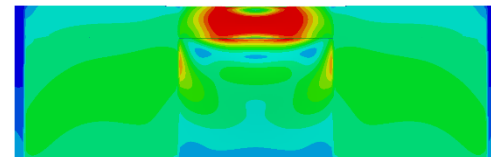
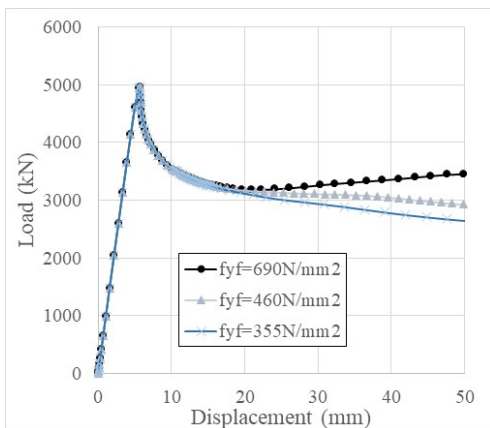


von Mises stresses at $F_{\max}=4033,1\text{ kN}$

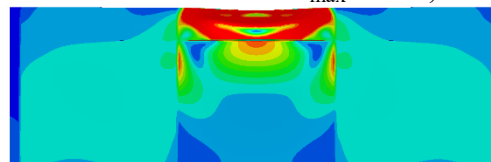


von Mises stresses at $\delta=50\text{mm}$

Figure 11. Unstiffened web. Stocky girders $t_w=15\text{mm}$

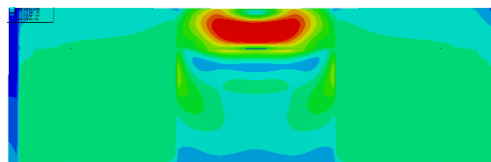
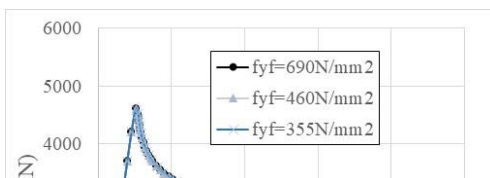


von Mises stresses at $F_{\max}=4951,7\text{ kN}$

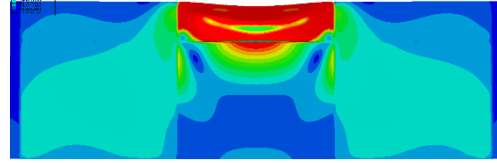


von Mises stresses at $\delta=50\text{mm}$

Figure 12. $b_1=400\text{mm}$. Stocky girders $t_w=15\text{mm}$

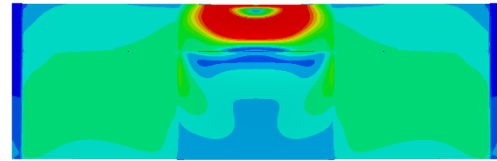
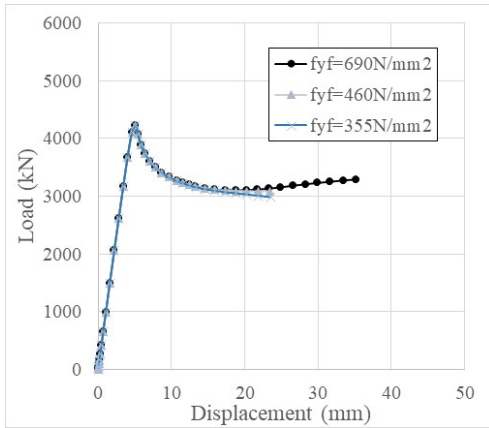


von Mises stresses at $F_{max}=4600,1$ kN

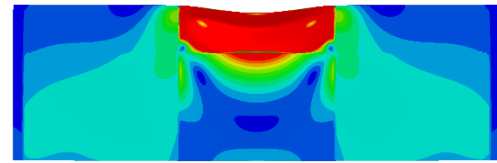


von Mises stresses at $\delta=50$ mm

Figure 13. $b_1=500$ mm. Stocky girders $t_w=15$ mm



von Mises stresses at $F_{max}=4224,5$ kN



von Mises stresses at $\delta=50$ mm

Figure 14. $b_1=600$ mm. Stocky girders $t_w=15$ mm

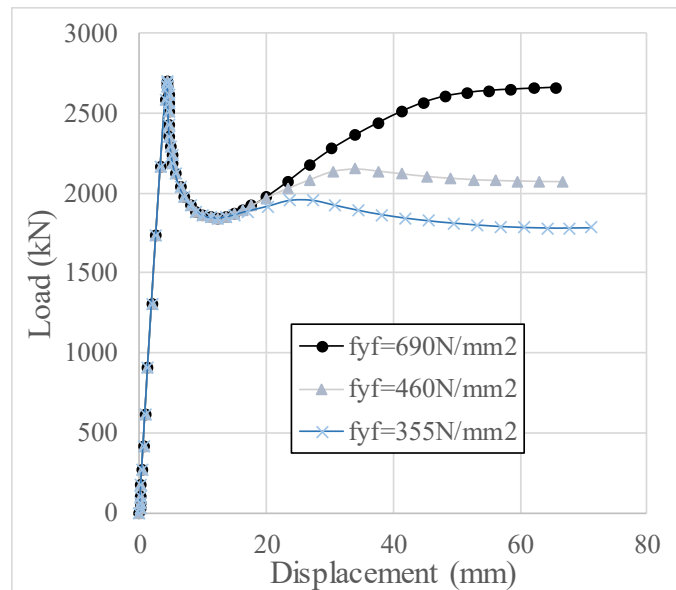


Figure 15. $b_1=400$ mm. Intermediate h_w/t_w

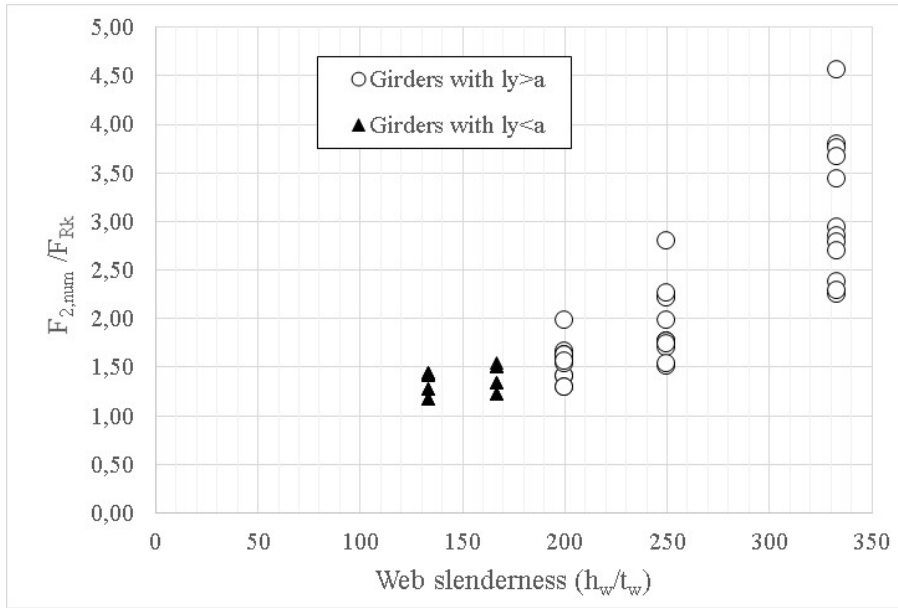


Figure 16. $F_{2,num}/F_{Rk}$ vs web slenderness

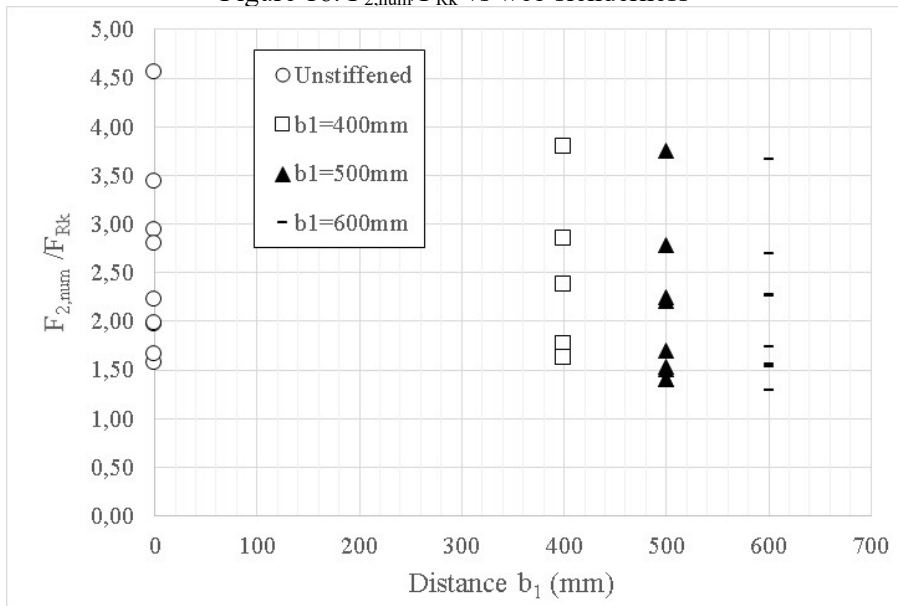


Figure 17. $F_{2,num}/F_{Rk}$ vs distance b_1

Table 1. Variations of the numerical study.

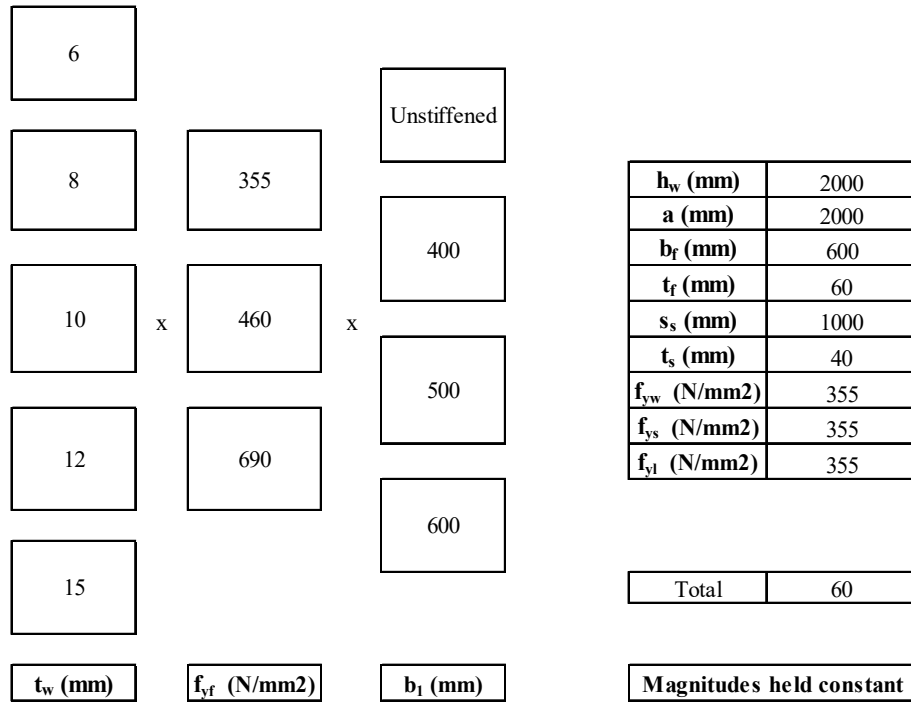


Table 2. EN1993-1-5 results for the set of unstiffened girders

Number	t _w (mm)	f _{yf} (N/mm ²)	I _{y,nv} (mm)	hw/tw	a/ly	I _{y,corrected} (mm)	k _F	F _{cr} (kN)	F _y (kN)	λ _F	Φ _F	χ _F	F _{Rk}	F _{RD}
U-1	6	355	2320,0	333,3	1,16	2000,0	8	163,3	4260,0	5,11	4,78	0,11	473,6	430,5
U-2	6	460	2320,0	333,3	1,16	2000,0	8	163,3	4260,0	5,11	4,78	0,11	473,6	430,5
U-3	6	690	2320,0	333,3	1,16	2000,0	8	163,3	4260,0	5,11	4,78	0,11	473,6	430,5
U-4	8	355	2159,2	250,0	1,08	2000,0	8	387,1	5680,0	3,83	3,66	0,15	840,0	763,6
U-5	8	460	2159,2	250,0	1,08	2000,0	8	387,1	5680,0	3,83	3,66	0,15	840,0	763,6
U-6	8	690	2159,2	250,0	1,08	2000,0	8	387,1	5680,0	3,83	3,66	0,15	840,0	763,6
U-7	10	355	2049,5	200,0	1,02	2000,0	8	756,0	7100,0	3,06	2,99	0,18	1309,3	1190,2
U-8	10	460	2049,5	200,0	1,02	2000,0	8	756,0	7100,0	3,06	2,99	0,18	1309,3	1190,2
U-9	10	690	2049,5	200,0	1,02	2000,0	8	756,0	7100,0	3,06	2,99	0,18	1309,3	1190,2
U-10	12	355	1968,5	166,7	0,98	1968,5	8	1306,4	8385,9	2,53	2,53	0,22	1865,5	1695,9
U-11	12	460	1968,5	166,7	0,98	1968,5	8	1306,4	8385,9	2,53	2,53	0,22	1865,5	1695,9
U-12	12	690	1968,5	166,7	0,98	1968,5	8	1306,4	8385,9	2,53	2,53	0,22	1865,5	1695,9
U-13	15	355	1878,9	133,3	0,94	1878,9	8	2551,5	10005,4	1,98	2,05	0,28	2834,9	2577,2
U-14	15	460	1878,9	133,3	0,94	1878,9	8	2551,5	10005,4	1,98	2,05	0,28	2834,9	2577,2
U-15	15	690	1878,9	133,3	0,94	1878,9	8	2551,5	10005,4	1,98	2,05	0,28	2834,9	2577,2

Table 3. EN1993-1-5 results for the set of girders with b₁=400mm

Number	tw (mm)	f _{yf} (N/mm ²)	l _y (mm)	hw/tw	a/l _y	l _{y,corrected} (mm)	k _F	F _{cr} (kN)	F _v (kN)	λ _F	Φ _F	χ _F	F _{RR}	F _{RD}
S-0.2-1	6	355	2320,0	333,3	1,16	2000,0	13,1	267,8	4260,0	3,99	3,80	0,14	605,3	550,3
S-0.2-2	6	460	2320,0	333,3	1,16	2000,0	13,1	267,8	4260,0	3,99	3,80	0,14	605,3	550,3
S-0.2-3	6	690	2320,0	333,3	1,16	2000,0	13,1	267,8	4260,0	3,99	3,80	0,14	605,3	550,3
S-0.2-4	8	355	2159,2	250,0	1,08	2000,0	13,1	634,8	5680,0	2,99	2,93	0,19	1072,7	975,2
S-0.2-5	8	460	2159,2	250,0	1,08	2000,0	13,1	634,8	5680,0	2,99	2,93	0,19	1072,7	975,2
S-0.2-6	8	690	2159,2	250,0	1,08	2000,0	13,1	634,8	5680,0	2,99	2,93	0,19	1072,7	975,2
S-0.2-7	10	355	2049,5	200,0	1,02	2000,0	13,1	1239,8	7100,0	2,39	2,41	0,24	1670,7	1518,8
S-0.2-8	10	460	2049,5	200,0	1,02	2000,0	13,1	1239,8	7100,0	2,39	2,41	0,24	1670,7	1518,8
S-0.2-9	10	690	2049,5	200,0	1,02	2000,0	13,1	1239,8	7100,0	2,39	2,41	0,24	1670,7	1518,8
S-0.2-10	12	355	1968,5	166,7	0,98	1968,5	12,9	2111,8	8385,9	1,99	2,06	0,28	2361,5	2146,8
S-0.2-11	12	460	1968,5	166,7	0,98	1968,5	12,9	2111,8	8385,9	1,99	2,06	0,28	2361,5	2146,8
S-0.2-12	12	690	1968,5	166,7	0,98	1968,5	12,9	2111,8	8385,9	1,99	2,06	0,28	2361,5	2146,8
S-0.2-13	15	355	1878,9	133,3	0,94	1878,9	11,8	3770,1	10005,4	1,63	1,74	0,34	3429,4	3117,7
S-0.2-14	15	460	1878,9	133,3	0,94	1878,9	11,8	3770,1	10005,4	1,63	1,74	0,34	3429,4	3117,7
S-0.2-15	15	690	1878,9	133,3	0,94	1878,9	11,8	3770,1	10005,4	1,63	1,74	0,34	3429,4	3117,7

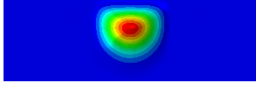
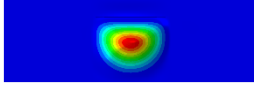
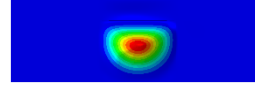
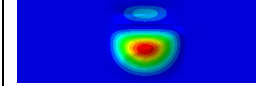
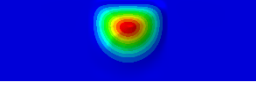
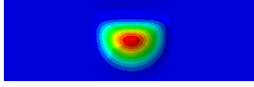
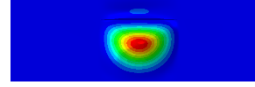
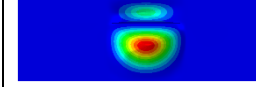
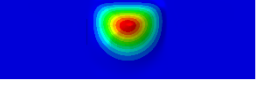
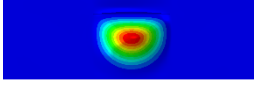
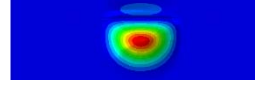
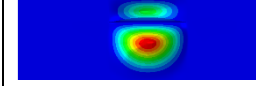
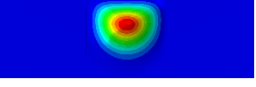
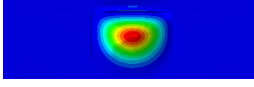
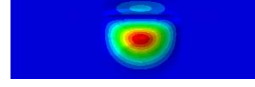
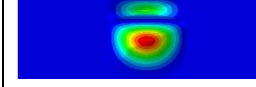
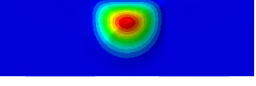
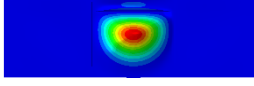
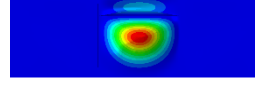
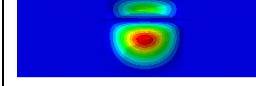
Table 4. EN1993-1-5 results for the set of girders with b₁=500mm

Number	tw (mm)	f _{yf} (N/mm ²)	l _y (mm)	hw/tw	a/l _y	l _{y,corrected} (mm)	k _F	F _{cr} (kN)	F _v (kN)	λ _F	Φ _F	χ _F	F _{RR}	F _{RD}
S-0.25-1	6	355	2320,0	333,3	1,16	2000,0	13,6	277,1	4260,0	3,92	3,74	0,14	615,6	559,6
S-0.25-2	6	460	2320,0	333,3	1,16	2000,0	13,6	277,1	4260,0	3,92	3,74	0,14	615,6	559,6
S-0.25-3	6	690	2320,0	333,3	1,16	2000,0	13,6	277,1	4260,0	3,92	3,74	0,14	615,6	559,6
S-0.25-4	8	355	2159,2	250,0	1,08	2000,0	13,6	656,8	5680,0	2,94	2,89	0,19	1091,0	991,8
S-0.25-5	8	460	2159,2	250,0	1,08	2000,0	13,6	656,8	5680,0	2,94	2,89	0,19	1091,0	991,8
S-0.25-6	8	690	2159,2	250,0	1,08	2000,0	13,6	656,8	5680,0	2,94	2,89	0,19	1091,0	991,8
S-0.25-7	10	355	2049,5	200,0	1,02	2000,0	13,6	1282,8	7100,0	2,35	2,37	0,24	1698,9	1544,5
S-0.25-8	10	460	2049,5	200,0	1,02	2000,0	13,6	1282,8	7100,0	2,35	2,37	0,24	1698,9	1544,5
S-0.25-9	10	690	2049,5	200,0	1,02	2000,0	13,6	1282,8	7100,0	2,35	2,37	0,24	1698,9	1544,5
S-0.25-10	12	355	1968,5	166,7	0,98	1968,5	13,6	2216,7	8385,9	1,95	2,01	0,29	2418,2	2198,3
S-0.25-11	12	460	1968,5	166,7	0,98	1968,5	13,6	2216,7	8385,9	1,95	2,01	0,29	2418,2	2198,3
S-0.25-12	12	690	1968,5	166,7	0,98	1968,5	13,6	2216,7	8385,9	1,95	2,01	0,29	2418,2	2198,3
S-0.25-13	15	355	1878,9	133,3	0,94	1878,9	13,0	4147,6	10005,4	1,55	1,67	0,36	3592,0	3265,5
S-0.25-14	15	460	1878,9	133,3	0,94	1878,9	13,0	4147,6	10005,4	1,55	1,67	0,36	3592,0	3265,5
S-0.25-15	15	690	1878,9	133,3	0,94	1878,9	13,0	4147,6	10005,4	1,55	1,67	0,36	3592,0	3265,5

Table 5. EN1993-1-5 results for the set of girders with b₁=600mm

Number	tw (mm)	f _{yf} (N/mm ²)	l _y (mm)	hw/tw	a/l _y	l _{y,corrected} (mm)	k _F	F _{cr} (kN)	F _v (kN)	λ _F	Φ _F	χ _F	F _{RR}	F _{RD}
S-0.3-1	6	355	2320,0	333,3	1,16	2000,0	13,1	268,0	4260,0	3,99	3,80	0,14	605,5	550,4
S-0.3-2	6	460	2320,0	333,3	1,16	2000,0	13,1	268,0	4260,0	3,99	3,80	0,14	605,5	550,4
S-0.3-3	6	690	2320,0	333,3	1,16	2000,0	13,1	268,0	4260,0	3,99	3,80	0,14	605,5	550,4
S-0.3-4	8	355	2159,2	250,0	1,08	2000,0	13,1	635,1	5680,0	2,99	2,93	0,19	1073,0	975,5
S-0.3-5	8	460	2159,2	250,0	1,08	2000,0	13,1	635,1	5680,0	2,99	2,93	0,19	1073,0	975,5
S-0.3-6	8	690	2159,2	250,0	1,08	2000,0	13,1	635,1	5680,0	2,99	2,93	0,19	1073,0	975,5
S-0.3-7	10	355	2049,5	200,0	1,02	2000,0	13,1	1240,5	7100,0	2,39	2,41	0,24	1671,2	1519,2
S-0.3-8	10	460	2049,5	200,0	1,02	2000,0	13,1	1240,5	7100,0	2,39	2,41	0,24	1671,2	1519,2
S-0.3-9	10	690	2049,5	200,0	1,02	2000,0	13,1	1240,5	7100,0	2,39	2,41	0,24	1671,2	1519,2
S-0.3-10	12	355	1968,5	166,7	0,98	1968,5	13,1	2143,6	8385,9	1,98	2,04	0,28	2378,8	2162,6
S-0.3-11	12	460	1968,5	166,7	0,98	1968,5	13,1	2143,6	8385,9	1,98	2,04	0,28	2378,8	2162,6
S-0.3-12	12	690	1968,5	166,7	0,98	1968,5	13,1	2143,6	8385,9	1,98	2,04	0,28	2378,8	2162,6
S-0.3-13	15	355	1878,9	133,3	0,94	1878,9	13,1	4186,7	10005,4	1,55	1,67	0,36	3608,4	3280,4
S-0.3-14	15	460	1878,9	133,3	0,94	1878,9	13,1	4186,7	10005,4	1,55	1,67	0,36	3608,4	3280,4
S-0.3-15	15	690	1878,9	133,3	0,94	1878,9	13,1	4186,7	10005,4	1,55	1,67	0,36	3608,4	3280,4

Table 6. Elastic buckling modes and shapes for the 1st Eigenvalue

t_w (mm)	Unstiffened	$b_1=400$ mm	$b_1=500$ mm	$b_1=600$ mm
6				
	$F_{cr}=237,2$ kN	$F_{cr}=411,6$ kN	$F_{cr}=477,6$ kN	$F_{cr}=552,8$ kN
8				
	$F_{cr}=550,6$ kN	$F_{cr}=937,6$ kN	$F_{cr}=1077,0$ kN	$F_{cr}=1193,8$ kN
10				
	$F_{cr}=1056,4$ kN	$F_{cr}=1753,4$ kN	$F_{cr}=1979,2$ kN	$F_{cr}=2097,4$ kN
12				
	$F_{cr}=1795,6$ kN	$F_{cr}=2910,8$ kN	$F_{cr}=3210,2$ kN	$F_{cr}=3317,4$ kN
15				
	$F_{cr}=3421,2$ kN	$F_{cr}=5410,0$ kN	$F_{cr}=5842,6$ kN	$F_{cr}=5893,8$ kN